J. COMBIN. MATH. COMBIN. COMPUT. 127b (2025) 8815--8832

Journal of Combinatorial Mathematics and Combinatorial Computing
www.combinatorialpress.com/jcmcc

Design of low-latency communication network for power system automation based on 5G technology

Yabin Chen[1], Wei Xu[1], Xiaoyu Deng[1], Yu Sui[1,✉]

[1] *Power Grid Planning Research Center of Guangdong Power Grid Co., Ltd., Guangzhou, Guangdong, 510220, China*

ABSTRACT

With the construction and development of new power system, grid business presents high reliability, high security protection, high flexibility, massive access level characteristics, 5G as the frontier technology of wireless network access, with high speed, wide connectivity, low latency features and advantages, and diversified grid business communication needs are highly compatible. Based on the characteristics of 5G communication technology, this paper analyzes its practicality in the power system. The main two protocols of the current autonomous network routing protocol for power system are proposed, and the inter-cluster routing optimization of OLSR is carried out by using AO algorithm. Simulate the predation behavior of skyhawk, develop the search strategy in the optimization process of AO algorithm, and construct the mathematical model of AO optimization algorithm. A quasi-inverse solution is used on the basis of the inverse solution to further increase the population diversity and convergence speed of the AO algorithm, while an adaptive weight factor strategy is used to balance the global search and local exploration capabilities of the AO algorithm. Simulation experiments are utilized to investigate the performance of the IAO algorithm as well as the PDR and delay in the mobile scenario of the power system. Comparing the PDR of the three protocols at different expected delivery distances, IOLSR still maintains a delivery rate of about 28% at a distance of 350m-500m. The optimized IOLSR shows further reduction in delay compared to OLSR in most of the cases with an average delay of 10829.43ns.

Keywords: 5G communication technology, AO algorithm, OLSR routing protocol, delivery rate, low latency

1. Introduction

The perfection of the market economy and the development of social economy makes the electric power enterprise also change the operation mode, from the production type gradually turned to the production and management type, which also makes the electric power enterprise join the wave of

✉ Corresponding author.
E-mail address: SuiYu202412@126.com (Y. Sui).
Received 20 March 2024; Revised 05 June 2024; Accepted 20 November 2024; Published Online 16 April 2025.
DOI: 10.61091/jcmcc127b-484

the information age. Power system automation technology plays a very important role in electric power enterprises, and with the continuous and profound development of information technology, the power system and electric power enterprises will gradually form their own power system automation network construction, so as to create good conditions for the development of the power system and electric power enterprises [1-3].

Power system automation network design process is, in the center of the power system to place the computer, the use of advanced information technology to the surrounding system for network radiation, in the substation around this, the power grid is to carry out the information set up and placement of monitoring devices, so that real-time monitoring, and ultimately the formation of an all-round network coverage, to ensure that the power system can be communicated within the information transmission and transmission [4-5]. Power system automation technology network design when the use of advanced computers for the overall scheduling, set up monitoring equipment is the operation and the work process of the fault, information recording and processing, and the preparation of reports and system operation and restoration of real-time control and monitoring. On this basis, networking can be used for the combined use of hardware and software, which can achieve greater automation and effectiveness of the power system [6-8].

Literature [9] develops a detailed description of smart grids and states that the integration of information and communication technologies with smart grids allows for better asset and energy management. It also discusses the various areas of communication and information technology involved in smart grid automation. Literature [10] describes a multi-stage planning model that considers all the key hard and software infrastructures of a distribution automation system with the aim of providing a methodology for distribution automation system planning. The methodology is also evaluated through testing and the results obtained are discussed. Literature [11] discusses distribution planning, performance calculations and protection to meet specific performance objectives. A business case for distribution automation and a methodology for calculating the benefits are illustrated based on an example study. The importance of tools such as data analytics for distribution network management is emphasized, showing that automation solutions tailored to individual needs can be achieved through the control and automation of distribution systems. Literature [12] aims to quantify the improvement of reliability metrics by automation of secondary substations. By applying the methodology in a real distribution network, the results point out that the value of this indicator has a significant impact on the revenues of the distribution network operator, which informs the strategic development of the distribution network. Literature [13] proposes framework components for power systems, communication networks, and automation networks for cybersecurity assessment of PSA. Risk assessment and mitigation measures against all demonstrated attacks are outlined by evaluating aspects such as cybersecurity and scalability issues of VOTNet. Literature [14] explores distribution automation and its distribution automation system in the context of the structure of distribution automation networks, by examining the functions and processing of distribution automation so as to select the appropriate communication method for implementation. The network with more bytes such as 64 bytes, 128 bytes and 256 bytes was also tested. Literature [15] proposes a multi-intelligence based network security enhanced distribution automation system and identifies its anomalies through multi-intelligence based network attack detection and mitigation algorithms. New integrated tools are proposed to detect and mitigate cyber intrusions in distribution networks by validating them in a testbed. Literature [16] discusses the main factors that hinder the implementation of automation in MV distribution networks and analyzes the regulatory impact. Based on a case study, it was pointed out that the structural characteristics are similar to those of European distribution networks. Therefore, general conclusions that are generally applicable to European distribution networks are obtained. Literature [17] not only discusses the practice of automation and control of large power systems, dynamics and control of power transmission systems, but also presents recent research results. The key challenges of dynamics, power system automation, etc., arising from the integration of renewable energy power plants are addressed. Literature [18] describes strategies for cost-effective ADAS implementation and evaluation. A locally centered FLISR based architecture is implemented in an urban underground MV distribution network and the complete procedure and structure of LC-FLISR is given. The results show that automated networks with reduced reliability metrics and ADAS have very high benefits. Literature [19] systematically describes the distributed grid automation system and emphasizes the importance of evaluating this system. Its ability to enhance the reliability calculation of the power system, including fault detection, restoration techniques, etc., is included. The impact of these enhancements on the reliability indices oriented to users and distributed generators is also interpreted and elaborated using the example of medium voltage networks.

This paper explores the application of 5g communication technology in power system and combs the characteristics of 5G communication technology. Based on this, OLSR protocol and AODV are proposed respectively, and an AO-based OLSR inter-cluster routing optimization scheme is analyzed. The biological behavior of predation by skyhawks is described, and the hunting behaviors adopted by skyhawks facing different prey are mathematically modeled by simulating them, and four different positional updating strategies are proposed, namely, expanding exploration, narrowing the search range, expanding exploitation, and narrowing exploitation. In order to solve the problems of the AO algorithm, such as weak local search ability and poor anti-stagnation ability, the quasi-inverse solution is used on the basis of the inverse solution to establish an elite inverse learning model. Meanwhile, in order to balance the global search and local exploration ability of the AO algorithm, the adaptive weight factor strategy is introduced in the pre iteration of the algorithm. Simulation experiments are conducted to verify the optimization effect of the IAO algorithm for OLSR routing protocols and the low latency situation applied in power systems.

2. 5G low-latency communication network design for new power systems

2.1. Application of 5G communication technology in power system

2.1.1. Analysis of 5G communication technology. The emergence of 5G communication technology is a major change in the field of communication, and its impact is far-reaching and significant [20]. From 1G-4G, China is mainly a user of related communication technologies, paying high patent fees. And 5G communication technology is mainly developed by China's Huawei, marking the leaping development of China's communication technology. For 5G communication technology, it has the following characteristics:

1) 5G communication high transmission rate. 4G era communication transmission rate is Mb/s level, for the daily user network needs can be basically satisfied. But with the rapid development of image technology, 4K, 8K and other ultra-high-definition video technology put into use. 4G communication technology obviously can not meet the demand. 5G communication transmission rate is Gb/s level, for ultra-high-definition video and other Gb-level files, can realize data download in seconds, greatly improving the user experience.

2) Low latency. Low latency is another feature of 5G communication technology, and the latency rate of 5G technology can reach within 10ms. The delay rate is greatly reduced, users can realize remote precision control, unmanned driving, AR technology and other new technologies, providing higher convenience for human beings.

3) High capacity: 5G communication technology has 100 times higher capacity than 4G communication technology. For ordinary users, voice calls in crowded areas will not be interfered with, thus ensuring the normal use of users. With the in-depth development of the Internet of Things (IoT) technology, the interconnection of everything has become the trend of the future. Traditional communications services are mainly for people. The use of the Internet of things, objective objects can also enter the mobile communication network, to achieve the function of sending and receiving

data, so that the number of mobile interconnections will show geometric growth. Existing 4G communication network due to limited user capacity, a large number of data users surge, will inevitably cause network congestion occurs, and ultimately manifests itself in a significant decline in user data transmission rate, high latency, and in serious cases, the base station crash phenomenon.

2.1.2. Application of 5G communication technologies. The application scenarios of 5G communication technology are categorized into 3 types: enhanced mobile broadband (eMBB), ultra-high reliable low-latency communication (u RLLC), and massive machine type communication (m MTC), as shown in Fig. 1. While eMBB focuses on enhancing the user experience, m MTC and uRLLC are designed to provide innovative solutions for industrial applications.

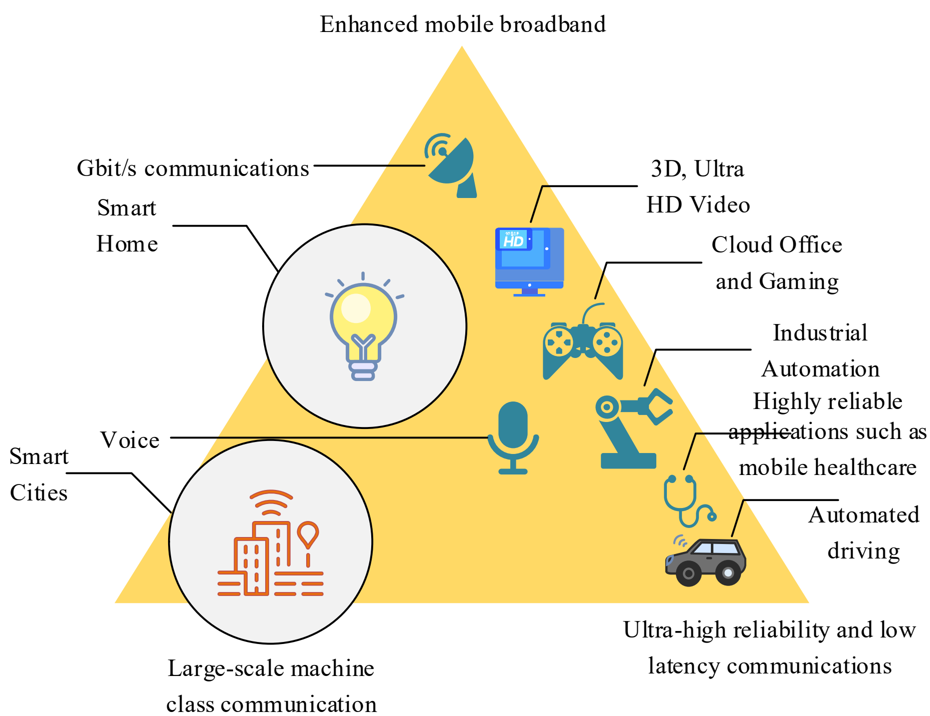

Fig. 1. Three application scenarios of 5G

The high reliability and low latency of 5G communication technology can support the real-time transmission of massive data, providing good conditions for distributed energy access in the field of renewable energy generation. Through 5G network, real-time monitoring, data analysis and remote control of PV power plant can be realized, which greatly improves the operation and maintenance efficiency and management level. Using the high-speed transmission capability of 5G communication technology, the massive data generated by PV power plants can be quickly uploaded to the cloud, and through big data analysis, real-time monitoring and prediction of power generation efficiency, equipment status, etc., can realize preventive maintenance and fault warning. Hebei Zhangjiakou power grid to Guyuan County kiln ditch village station as a pilot, with the help of operators to build industrial-level 5G security network, the use of localized security protocol technology, to solve the main control box and sub-control box between the security communication problems, distributed photovoltaic station and the main station of the communication delay is reduced to 20ms within the signal transmission blind zone, low cost and high reliability to achieve the master station of the distributed photovoltaic power station data collection and remote control, real-time data collection and remote control. It realizes real-time data collection and remote control of distributed photovoltaic power station from dispatching master station at low cost and with high reliability, as well as the observable, measurable, adjustable and controllable on-site equipments by smart grid dispatching technology support system.

2.2. AO-based inter-cluster routing optimization for OLSRs

2.2.1. OLSR routing protocols. Currently there are two main protocols for power system self-organizing network routing protocols, which are a priori routing protocols and reactive routing protocols.OLSR protocol is a typical a priori routing protocol, that is, it will store the routing information in advance, and the nodes only need to send the data directly when communicating [21]. It is characterized by low latency and is suitable for dense scenarios with a large number of nodes.The OLSR protocol is mainly divided into the following three steps.

Step 1: Neighbor Sensing: In OLSR protocol, the communication between nodes needs to ensure that both sides are symmetric links. In order to find nearby "neighbors", nodes in the network broadcast HELLO messages every two seconds. One of the nodes is an asymmetric neighbor if it is able to receive the message transmitted by the other node. If you can meet in a certain period of time and another node to do three handshakes, that is, both sides received HELLO messages are found in the symmetric part of the message contains their own information, then the two nodes are each other's symmetric neighbors, the link between the nodes is a symmetric link can be communicated.

Step 2: MPR mechanism. The node selects some of the neighboring nodes as its relay nodes and only the selected relay nodes are able to forward the control messages of the node.The MPR node will broadcast the TC message to the nearby nodes every 5 seconds and the message mainly includes the MPR node information.The MPR node will continuously flood the message to all the nodes in the whole network.

Step 3: Routing Calculation.The OLSR protocol uses Dijkstra routing to calculate the shortest route required to the target node. A comprehensive study found that the existing OLSR protocol has the following problems: (1) The network topology changes too quickly, the link is easy to break, and the data is retransmitted resulting in lower efficiency. (2) Low success rate or high packet loss rate of data sending, resulting in higher latency. (3) Routing path selection algorithm is more single, resulting in higher overhead and affecting transmission efficiency.

2.2.2. AODV routing protocols. Also in the network application scenario of power systems, a low delay AODV routing protocol (LD-AODV) has been designed [22]. The algorithm introduces a link quality judgment mechanism to discover the optimal route in the route discovery process, as a way to improve the route quality. This mechanism mainly adopts signal strength cumulative percentage approach, while realizing the limitation of unreliable paths and hops, but there is a problem with this approach, that is, the judgment of each node based on the signal strength cumulative percentage approach only is too rough, which may lead to the existence of a large number of hops but the path is reliable options do not have the opportunity to send, resulting in route loss and other problems.

Moreover, the definition of signal strength does not correspond to PER, which is usually a linear function of RSSI. The combination of these reasons leads to its selection of links that remain unreliable.

Therefore the improved algorithm considers delay, hop count and cascade P_{rr} and lets node i (assuming that it sends to node j) make the choice of whether to transmit or not, and the transmit probability P is given in the following equation:

$$P = P_{rr_{Lot}} \times \Pr r_{ij} \times W\left(N_{Laxt}\right) \tag{1}$$

where: $P_{rr_{Lot}} = \prod_{n} P_{rr} r_{jn}$ denotes the cumulative success rate of sending packets from the source node to node j, Prr_{ij} denotes the success rate of sending packets from node i to node j, and N

denotes the number of hops experienced from the source node to the nearest j node. W is the weighting factor corresponding to the number of hops, which is given by Eq:

$$W = \max\left(N - En, 0\right)^{\alpha} \quad (2)$$

where: En denotes the desired average hop count, and α denotes the empirical value coefficient, which is taken as 0.25 to ensure that the larger the hop count the smaller the forwarding probability. Where the average hop count can be adjusted according to the communication situation and distance. Prr is the average packet sending success rate, which is estimated based on RSSI and channel noise magnitude, as well as packet length (packet length is chosen as the empirical value that best suits the scenario), and the specific formula is:

$$P_{rr} = \left(1 - Ber\right)^{k} \quad (3)$$

Where: k denotes the packet length bit, Ber is the bit error rate.

The bit error rate Ber of frequency shift keying FSK is calculated as:

$$Ber = Q\sqrt{\frac{E_o}{N_o}} \quad (4)$$

where: Q function is the Gaussian error function, also known as the Q value, E_b is the bit energy and N_0 is the noise power spectral density.

The final destination node uses both parts of the threshold to make a judgment in routing, where the first part is $P_{rr} > 0.7$ and the second is the above mentioned P to make a choice to use a path that is shorter and has a higher launch success rate.

2.3. AO algorithm

By analyzing the update strategy of the Skyhawk optimization algorithm, it can be seen that the AO algorithm has strong global exploration ability and fast convergence speed, but the global search process occupies too many cycles, while the population diversity is poor in the late stage of the algorithm, which leads to the weak local search ability of the algorithm, poor anti-stagnation ability, and easy to fall into the local optimum in the complex optimization problem. Aiming at the deficiencies of the AO algorithm, this chapter proposes an improved eagle optimization algorithm (IAO) to improve the convergence rate of the algorithm and the accuracy of the search for optimal, which lays the foundation for the later optimization of the wind power and photovoltaic output combination prediction model and the new type of optimal scheduling of the electric power system considering the minimum inertia constraints.

2.3.1. Description of Predation Behavior of the Skyhawk. Skyhawk is a kind of raptor in North America, with faster flight speed, high agility, sharp and strong claws and unique predation methods, its hunting objects include squirrels, hares, ground animals such as groundhogs and small fish floating at sea level. According to the different hunting objects, the skyhawk will flexibly choose the predation strategy, and its common predation behavior has four kinds, namely, high-flying swooping to prey on flying birds, short-distance gliding to attack squirrels or seabirds, low-flying and slow descending to capture slow-moving prey such as turtles and rattlesnakes, etc., and swooping or walking on land to catch prey such as deer, etc., the skyhawk optimization algorithm position updating strategy inspired by the skyhawk's predatory behavior, which can be based on the number of iterations and the value of the random number to choose the update strategy.

2.3.2. Mathematical model construction for AO optimization algorithm. The search strategy in the optimization process of the AO algorithm is developed by simulating the predatory behavior of the skyhawk in the face of different prey, and the predatory process of the skyhawk maps the algorithm's process of finding out the optimal solution from the candidate solutions, and the capture of the agile prey can reflect the global search capability of the algorithm, and the predation of the slow-moving prey reflects the local exploration capability of the algorithm. The algorithm performs mathematical modeling by simulating the hunting behaviors adopted by the skyhawk in the face of different prey, and proposes four different location updating strategies, which are described as follows:

1) Expanded Exploration $\left(X_1\right)$. In the first hunting behavior $\left(X_1\right)$, the skyhawk recovers the location of the prey, then soars high in the sky to select the best prey area, followed by a dive to capture the prey. The mathematical model of this behavior can be represented by Equation (5):

$$X_1(t+1) = X_{best}(t) \times \left(1 - \frac{t}{T}\right) + \left(X_M(t) - X_{best}(t)\right) \times rand \tag{5}$$

$$X_M(t) = \frac{1}{N} \sum_{i=1}^{N} X_i(t) \forall j = 1, 2, L, \dim \tag{6}$$

where, t represents the current algorithm optimization number, T represents the total algorithm optimization number, $X_{best}(t)$ represents the optimal hunting position under the current optimization number t, $X_1(t+1)$ represents the next solution generated t under the first hunting behavior $\left(X_1\right)$, $rand$ takes a random number from $[0,1]$, $X_M(t)$ represents the average value of the solution under the current t iteration, N represents the number of candidate solutions, and dim represents the dimensionality of the problem being optimized.

2) Narrowing the search $\left(X_2\right)$. In the second hunting behavior $\left(X_2\right)$ the skyhawk discovers the location of the prey and hovers over it in preparation for catching the target, this strategy of the skyhawk is called the short gliding attack with isometric flight. The mathematical model of this behavior can be represented by equation (7):

$$X_2(t+1) = X_{best}(t) \times Levy(D) + X_R(t) + (y - x) \times rand \tag{7}$$

where $X_2(t+1)$ denotes the next solution of t generated under the second hunting behavior $\left(X_2\right)$, $Levy\left(D\right)$ denotes the Lévy flight distribution function computed using Eq. (7), $X_R(t)$ denotes the random solution drawn from $\left[1, N\right]$, and x and y are the parameters controlling the shape of the spiral search computed in Eq. (8):

$$\begin{cases} Levy(D) = s \times \dfrac{u \times \sigma}{|v|^{\frac{1}{\beta}}} \\ \sigma = \left(\dfrac{\Gamma(1+\beta) \times \sin\left(\dfrac{\pi\beta}{2}\right)}{\Gamma\left(\dfrac{1+\beta}{2}\right) \times \beta \times 2^{\left(\frac{\beta-1}{2}\right)}} \right) \end{cases} \tag{8}$$

where s takes 0.01, u, v can take any value in $[0,1]$, β takes 1.5, and $\Gamma(x)$ represents the gamma function:

$$\begin{cases} x = r \times \sin(\theta) \\ y = r \times \cos(\theta) \\ r = r_1 + 0.00565 \times D_1 \\ \theta = -\omega \times D_1 + \dfrac{3 \times \pi}{2} \end{cases} \tag{9}$$

where ω is taken as 0.005, r_1 is taken as the number of search cycles between [1, 20], and D_1 is taken as an integer in $[1, dim]$.

3) Extended exploitation (X_3). In the third hunting behavior (X_3), the skyhawk discovers slower-moving prey such as turtles and rattlesnakes, etc., and after determining the hunting area, the skyhawk approaches the prey in low altitude and slow flight or prepares to land and attack the prey. The mathematical model of this behavior can be represented by equation (10):

$$\begin{aligned} X_3(t+1) = &\left(X_{best}(t) - X_M(t)\right) \times \alpha - rand \\ &+((UB - LB) \times rand + LB) \times \delta \end{aligned} \tag{10}$$

where $X_3(t+1)$ denotes the next solution of t generated under the third hunting behavior (X_3), α, δ are taken as 0.1, LB, UB are the upper and lower bounds of the optimized problem.

4) Reduced development (X_4). In the fourth hunting behavior (X_4), the skyhawk approaches the prey and launches an attack, adjusting its position to capture the prey based on the prey's random escape response. The mathematical model of this behavior can be represented by equation (11):

$$\begin{aligned} X_4(t+1) = &QF \times X_{best}(t) - \left(G_1 \times X(t) \times rand\right) \\ &- G_2 \times Levy(D) + rand \times G_1 \end{aligned} \tag{11}$$

where $X_4(t+1)$ denotes the next solution of t generated under the fourth hunting behavior (X_4), QF denotes the equilibrium function of the search strategy computed using Eq. (12), G_1 denotes the trajectory of the skyhawk's action when it grabs the prey computed using Eq. (13), and G_2 denotes the slope of the skyhawk's flight between its starting position and its position at the time when it feeds on the prey computed using Eq. (14):

$$QF(t) = t^{\frac{2 \times rand - 1}{(1-T)^2}} \tag{12}$$

$$G_1 = 2 \times rand - 1 \tag{13}$$

$$G_2 = 2 \times \left(1 - \frac{t}{T}\right) \tag{14}$$

2.4. Improvement of the Skyhawk optimization algorithm

2.4.1. Elite reverse learning. Let the population size of the skyhawk be N and the dimension of the problem being optimized be d. The position vector of the i rd skyhawk in the d th dimension of the search space can be denoted as $X_i = \left(x_i^1, x_i^2, L, x_i^k, Lx_i^d\right)(i = 1, 2, LN)$, $x_i^k \in [LB_i, UB_i]$, and let $X_{io} = \left(x_{io}^1, x_{io}^2, L, x_{io}^k, Lx_{io}^d\right)$ be the inverse solution of X_i, where x_i^k corresponds to the inverse solution as follows:

$$x_{io}^k = UB_i + LB_i - x_i^k \tag{15}$$

In order to further increase the diversity of the population and the convergence speed, this paper adopts the method of quasi-inverse solution on the basis of inverse solution, and compares the fitness values of the randomly generated initial solution and its corresponding quasi-inverse solution, and takes the better one as the initial solution, and the quasi-inverse solution $\hat{x}_i$ corresponding to x_i^k is obtained by evolving on the basis of Eq. (16):

$$\hat{x}_i = \begin{cases} rand\left(avg_i, x_{io}^k\right), x_i^k \le avg_i \\ rand\left(x_{io}^k, avg_i\right), x_i^k > avg_i \end{cases} \tag{16}$$

where $avg_i = \left(UB_i - LB_i\right)/2$ and $rand\left(a,b\right)$ are random numbers generated between a and b.

Setting the problem to be solved as a minimization problem, the objective function is f, x_i^k, $\hat{x}_i$ are some random initial solution and its corresponding quasi-inverse solution respectively, if $f\left(\hat{x}_i\right) < f\left(x_i^k\right)$ is satisfied, replace x_i^k with $\hat{x}_i$, and vice versa, keep x_i^k as the initial population individual. It can be seen that the improved strategy only increases the complexity of the initialization process, does not change the size of the population, and does not increase the complexity of the later solution.

2.4.2.Adaptive Weighting Factor Strategy. In order to balance the global search and local exploration ability of the AO algorithm, in the early iteration of the algorithm, it is given larger and faster changing weights to strengthen the global expansion performance of the algorithm, and in the late iteration, it is given smaller and slower changing weights to reduce the possibility of the algorithm falling into the local optimum. In this paper, the adaptive weight factor strategy is introduced in the position update of the standard Skyhawk optimization algorithm, and the proposed adaptive weight factor calculation formula is as follows:

$$\begin{cases} \lambda = \exp^{\frac{1-t}{T-t+1}} \\ w = 2^{\lambda} - 1 \end{cases} \tag{17}$$

where t is the current iteration number and T is the total iteration number.

After the introduction of adaptive weight factors, the position update equations (5) and (11) are changed to equations (18) and (19).

$$X_1(t+1) = w \times X_{best}(t) + \left(X_M(t) - X_{best}(t)\right) \times rand \tag{18}$$

$$\begin{aligned} X_4(t+1) = QF \times X_{best}(t) - \left(G_1 \times X(t) \times rand\right) \\ -2 \times w \times Levy(D) + rand \times G_1 \end{aligned} \tag{19}$$

2.5. Simulation verification of the improved algorithm

2.5.1. Delay analysis. Since it is difficult to calculate the decomposition delay for k matrix column by a formula, the simulation is carried out in this paper by using Matlab software, and its simulation results are shown in Fig. 2. In the figure, IAO1 denotes the IAO algorithm with parameter $k = 2$, N denotes the matrix size, and the delay PL is defined as the number of clock cycles between the first valid signal input and the first valid data output. When parameter $k = 1$, the IAO algorithm is the same as the conventional AO algorithm in terms of element elimination order, so the IAO1 curve represents the delay characteristics of the conventional AO algorithm. As shown in the figure, as the matrix size increases, the delay growth trend of the traditional AO algorithm is much larger than that of the IAO algorithm, for example, IAO and IAO8, the delay processing in the matrix of 120 are 12564.47964 and 3864.25339, respectively, so that the IAO algorithm proposed in this paper has a greater advantage of low latency in the wireless communication of the power system.

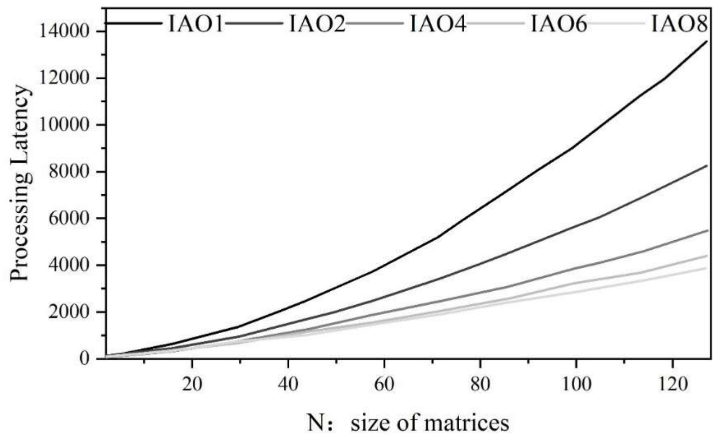

Fig. 2. Clock cycle delay of IAO algorithm

In order to quantitatively analyze the optimization effect of IAO algorithm on delay, Figure 3 shows the delay reduction efficiency of IAO algorithm with different parameters. As can be seen from Fig. 3, a better delay reduction effect can already be achieved when parameter $k=4$ is used, at which time the delay reduction efficiency can reach a maximum of 0.6. If we continue to increase the value of k, not only is the delay reduction effect not obvious, but it may also cause additional decoding errors, so in this chapter, $k=4$ is set as the default parameter of the IAO algorithm, and it is also used as the parameter setting for the hardware design in the later part of the paper.

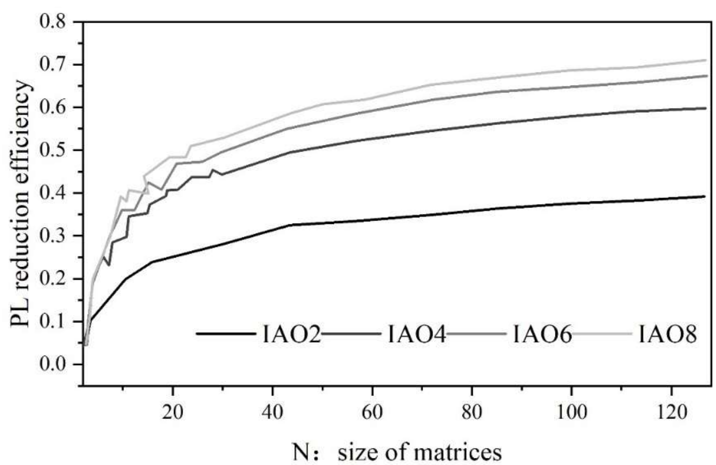

Fig. 3. The latency efficiency of the IAO algorithm of different parameters

2.5.2. Load Payload Changes. Fig. 4 shows the delay test data under different length loads. According to the experimental scheme of subnet delay test, the communication delays under different link rates are tested for data messages with different length data loads. The results are as follows: when the payload is within 512 bytes, the delay SDR and QDR intervals are between [1.34,1.9] and [0.4,0.47] respectively.

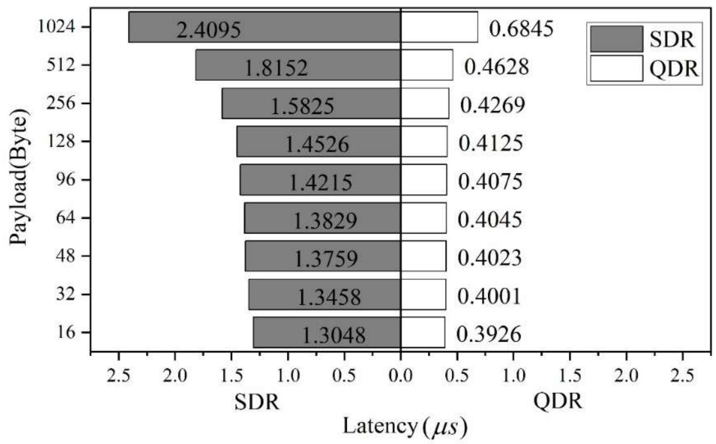

Fig. 4. Delayed test data under different length loads

In order to observe the trend of subnet communication delay performance more intuitively, the delay test is carried out under data load Payload variation and compared with AO algorithm experiments, and the results are plotted as follows. Fig. 5 shows the subnet communication delay variation, from which it can be seen that the subnet delay performance of IAO is significantly better than that of AO in the above subnet communication delay experiments. When the link rate is 10Gbps, the communication delay between two modules connected through the switch is less than 1 microsecond, between 0.3 and 0.7. The experimental results show that the IAO algorithm can not only successfully complete the connection of subnets, but also has excellent performance.The high efficiency of the IAO algorithm is attributed to the communication interface through direct connection, streamlined communication hierarchy and short message structure.

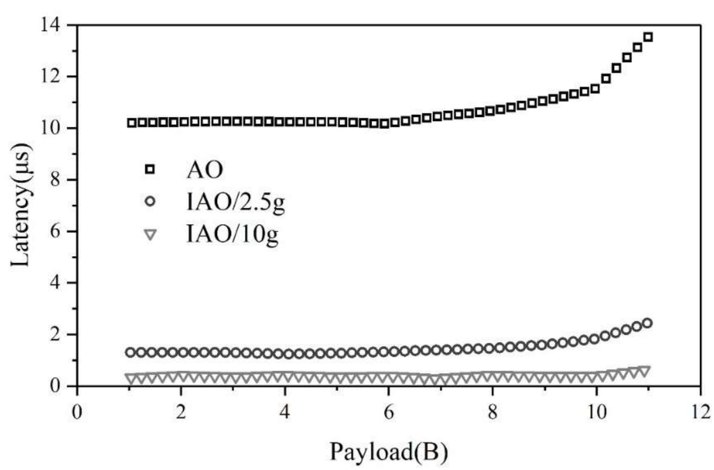

Fig. 5. Subnet communication delay change

3. Simulation experiments and analysis

3.1. Performance assessment indicators

3.1.1. Group delivery rate. Packet delivery rate (P_{dr}) is a very important factor in measuring the performance of routing protocols in any network. The performance of the protocol depends on the different parameters chosen for the simulation. The main parameters are packet size, number of nodes, transmission range and network structure. The packet delivery rate can be obtained by dividing the total number of data packets arriving at the destination by the total data packets sent from the source. In other words, the packet delivery rate is the ratio of the number of packets $\left(P_{revd}\right)$

received at the destination to the number of packets (P_{sd}) sent from the source. The higher the packet delivery ratio, the better the performance.

$$P_{dr} = P_{rad} / P_{sd} \tag{20}$$

3.1.2. Average inter-cluster end-to-end delay. The average inter-cluster end-to-end delay is the time it takes for a packet to be routed through the network from its source to its destination.

The average end-to-end delay can be obtained by calculating the average of the end-to-end delays of all successfully delivered messages. Thus, the end-to-end delay depends to some extent on the packet transmission rate. As the distance between source and destination increases, the probability of packet loss also increases. The average end-to-end delay includes all possible network delays, i.e., buffered route detection delay, MAC delay in retransmission, and delay in propagation and transmission. The average end-to-end delay is estimated as follows:

$$AD_{CE2E} = \frac{\sum_{i=1}^{n}(T_{ri} - T_{si})}{n} \tag{21}$$

where n is the number of successfully received packets in each second, T_{ri} denotes the timestamp at which the receiver received the packet, and T_{si} is the timestamp for the packet when the sender sends the ith packet. The calculated delay is the average delay in nanoseconds (ns) of received packets per unit time.

3.1.3. Control overhead. Control overhead is also referred to as normalized routing load (N_{rl}). Specifically, normalized routing load is the ratio of the number of control packets (P_c) that undergo data forwarding to the number of packets (P_{sd}) that are successfully transmitted in the network. The higher the normalized routing load, the higher the routing packet overhead and therefore the lower the protocol performance. N_{rl} is also referred to as the number of routing packets sent per packet delivered at the destination. Each routing transmission is counted hop by hop as one transmission. It is the sum of all control packets sent by all nodes in the network to discover and maintain routes.

$$N_{rl} = \frac{P_c}{P_{sd}} \tag{22}$$

3.2. *Performance Evaluation of Power System Mobile Scenarios*

In order to study the effect of node mobility on network performance, other parameters are fixed and only node mobility is varied. The network performance of the nodes is recorded under average speed conditions from 60km/h to 120km/h. In these scenarios, the number of nodes is fixed at 40 and the data rate is kept constant at 4 packets per second (16 Kbps). The objective is to check the network behavior of the optimized MOLSR, OLSR and AODV protocols under different mobility. The main parameters of these simulation scenarios are shown in Table 1.

Table 1. The main parameters of the mobile scenario simulation

Parameter	Value
Analog time	120s
Simulated area	300m*1500m
Number of nodes	40

Node velocity	60-120km/h
Phy/mac protocol	IEEE 802.11p
Expected transmission distance	50-500m
Routing protocol	OLSR,AODV,MOLSR
Transport layer protocol	UDP
Transmitting power	7.5dBm
Wireless signal loss model	Two Ray Ground

3.2.1. PDR for different expected delivery distances. Figure 6~Figure 8 shows the variation of AODV delivery with BSM transmission distance, OLSR delivery rate variation with BSM transmission distance, and IOLSR delivery rate variation with BSM transmission distance, respectively. As shown in Fig. 6~Fig. 8 compare the variation of delivery rate of different protocols at different speeds with different BSM unit distances (1 BSM unit distance=50m). It can be seen that OLSR, AODV, and IOLSR all have an inevitable and obvious drop in delivery rate as the expected transmission distance increases, and the PDR is already less than 50% at 200m expected transmission distance. This may be limited by the underlying protocols, scenarios, and the impact of the transmit power, after testing, increasing the transmit power can significantly improve the PDR over longer distances, this section only compares the impact of different speeds on the routing protocols, so the transmit setting is fixed at 7.5dBm.

After comparison, although all three protocols maintain a high PDR at 1 BSM unit distance and 2 BSM unit distance, at 3 BSM unit distance (150m), the PDR starts to decrease gradually due to the speed enhancement. Among them, both AODV and OLSR decreased significantly, but IOLSR still maintained a slightly higher delivery rate. And with the enhancement of BSM unit distance, IOLSR still maintains a delivery rate of about 28% at 7 to 10 unit distances (350m-500m).

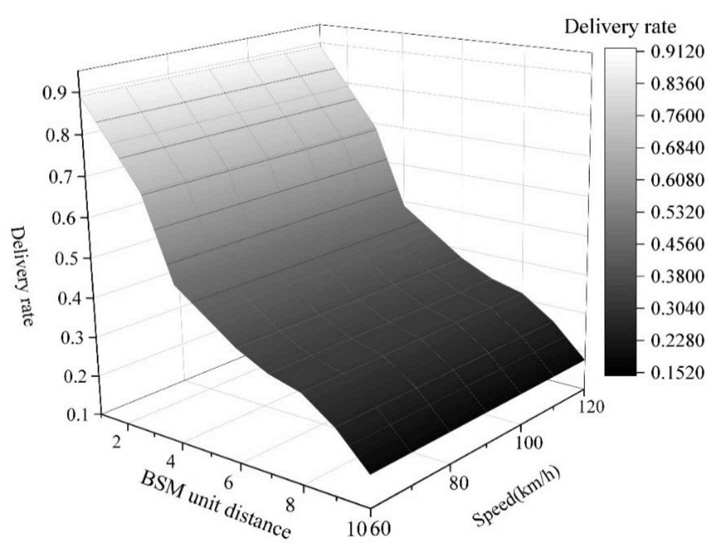

Fig. 6. The AODV changes the delivery of BSM distance

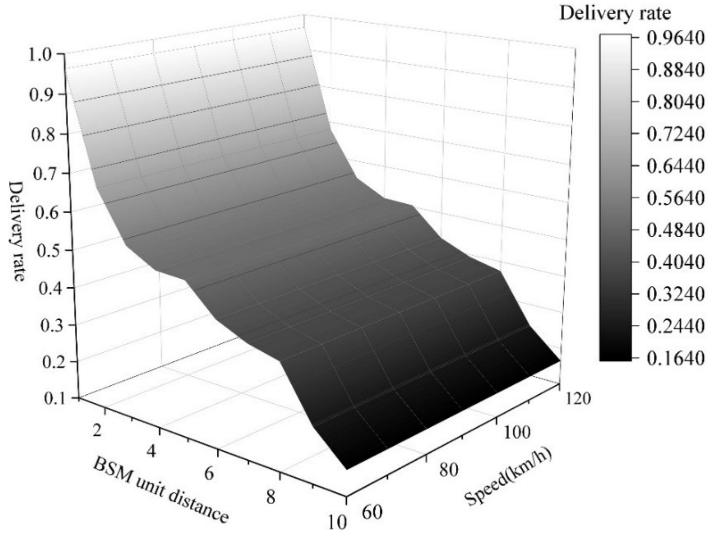

Fig. 7. OLSR changes the delivery rate of BSM distance

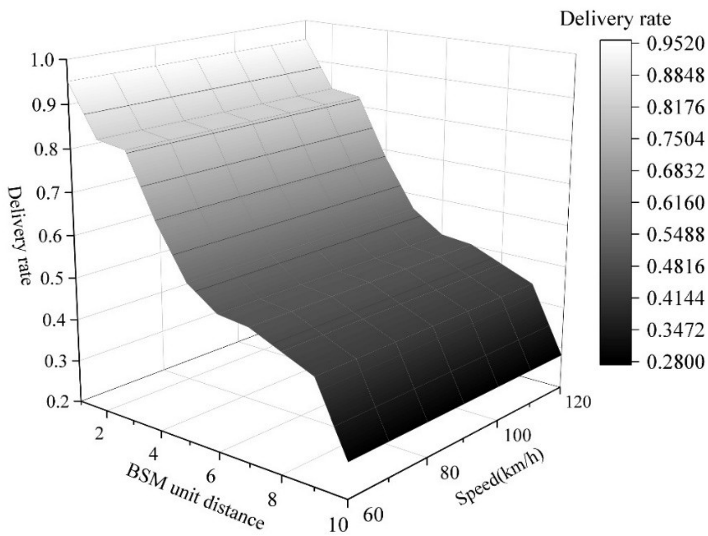

Fig. 8. IOLSR changes the delivery rate of BSM distance

3.2.2. PDR at 100km/h. Fig. 9 shows the PDR of the three protocols at 100km/h speed, Fig. (a) shows the variation of 100m transmission distance drop rate of the three protocols at 100km/h, and Fig. (b) shows the 150m transmission distance drop rate of the three protocols at 100km/h. It can be seen that at the beginning of the simulation, the drop rate of the three protocols all starts from 0 and climbs up gradually, which is because both OLSR and AODV need to be initialization for the route construction process. At the average speed of 100km/h, both AODV and OLSR maintain similar PDRs, but the IOLSR delivery rate is slightly higher than them, ranging from 0.68% to 0.91%. As can be seen in Fig. (b), IOLSR leads the other two protocols by a large margin, with a delivery rate range that stays above 0.58%. Taken together, the PDR improves in both the 2 BSM unit distance and 3 unit distance cases, which is due to the more accurate optimization of IOLSR for power system scenarios.

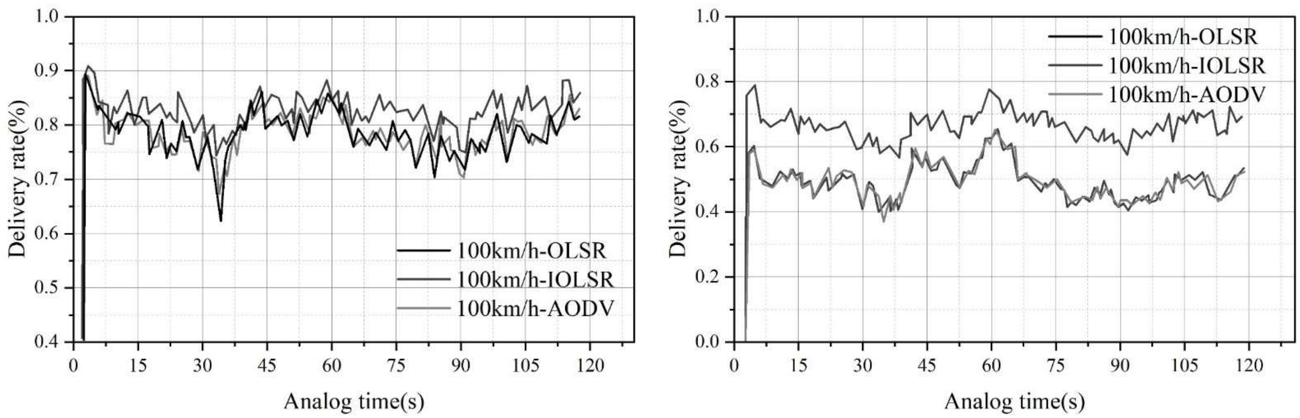

(a)100 m/h is 100 meters of transmission distance (b)100 m/h is 150 meters of transmission distance

Fig. 9. The three protocols are PDR at 100km/h

3.2.3. Overhead at different speeds. Figure 10 shows the speed versus average overhead relationship for the route control overhead, also known as normalized routing load. In this case, the percentage of AODV route control overhead gradually increases as the speed increases. While OLSR and IOLSR gradually decrease. It is worth noting that AODV consistently has a higher overhead than OLSR in this simulation scenario. The reason is that AODV is an on-demand routing protocol, which establishes routes only when they are needed. This means that AODV needs to initiate a new route discovery process whenever the network topology changes. In contrast, OLSR, as a link state protocol, exchanges link state information periodically, which makes the routing information more stable and up-to-date, thus reducing the overall control overhead in some scenarios. The network topology in the simulation environment changes frequently (e.g., high-speed moving nodes), and AODV may trigger route reconstruction frequently, thus increasing the route control overhead.OLSR can handle this dynamic environment more efficiently by updating periodically.IOLSR performs in between, with an overhead fluctuating around 33%. This explains why the AODV protocol overhead is instead higher than OLSR in this scenario.

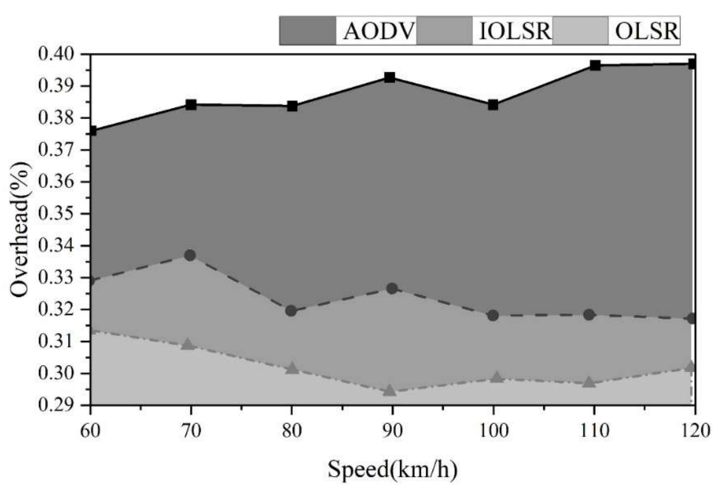

Fig. 10. Speed and average overhead relations

3.2.4. Delay at different speeds. Fig. 11 shows the average delay of nodes at different speeds. It can be seen that the optimized IOLSR has a further reduction in delay compared to OLSR in most cases. This is due to the fact that the parameters are tuned in such a way that they try to enhance the time interval of various periodic control messages used to maintain the routing table while keeping the rest of the network performance unchanged. Leaving other time schedules for non-control messages to be sent, this reduces the average delay, which is 10829.43ns.

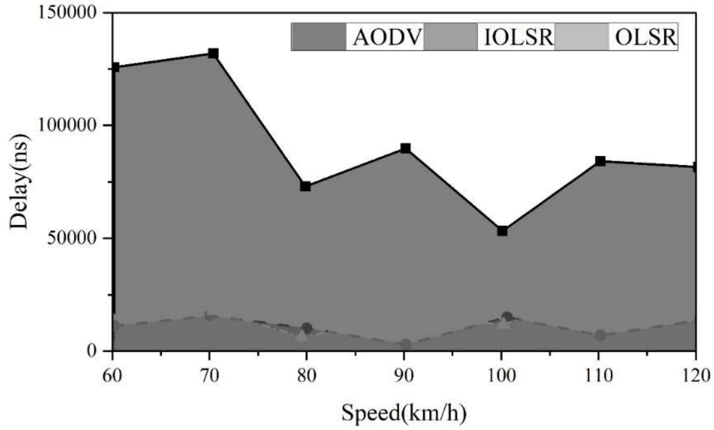

Fig. 11. Average delay of nodes at different speeds

4. Conclusion

Based on 5G communication technology, this paper proposes AO-based OLSR clusterware routing optimization, improves the AO algorithm and constructs the mathematical model of its optimization algorithm, and verifies the feasibility of the improved algorithm through simulation experiments. Based on the performance evaluation metrics, evaluate the delay, overhead and other metrics in the mobile scenario of the power system. Comparing the delay growth trend of AO algorithm and IAO algorithm, taking IAO and IAO8 as an example, the delay processed when the matrix is 120 is 12564.47964 and 3864.25339, respectively, and the optimized IAO algorithm has a large low-delay advantage in the wireless communication of power system. The delay reduction efficiency of IAO algorithm reaches up to 0.6 when parameter $k=4$ is used, so parameter $k=4$ is set as the default parameter of IAO algorithm in power systems. Meanwhile, when the link rate is 10Gbps, the communication delay between two modules connected through the switch under the IAO algorithm is lower than 1 microsecond, between 0.3 and 0.7. Comparing the relationship between different speeds and the average overhead, IOLSR performs between AODV and OLSR, with the overhead fluctuating around 33%, meanwhile, the average delay of IOLSR between speeds of 60 and 120km/h is 10829.43ns.

Funding

This work was supported by Special Topic 9 of Guangdong's "15th Five Year Plan" New Power System Planning: Research on Guangdong Power Grid's "15th Five Year Plan" Secondary System Planning (Project Number: 031000QQ00240021).

References

[1] Eltag, K., Aslamx, M. S., & Ullah, R. (2019). Dynamic stability enhancement using fuzzy PID control technology for power system. International Journal of Control, Automation and Systems, 17, 234-242.

[2] Khan, A. A., Laghari, A. A., Rashid, M., Li, H., Javed, A. R., & Gadekallu, T. R. (2023). Artificial intelligence and blockchain technology for secure smart grid and power distribution Automation: A State-of-the-Art Review. Sustainable Energy Technologies and Assessments, 57, 103282.

[3] Kumar, D. S., Savier, J. S., & Biju, S. S. (2020). Micro-synchrophasor based special protection scheme for distribution system automation in a smart city. Protection and Control of Modern Power Systems, 5(1), 1-14.

[4] Wójtowicz, R., Kowalik, R., & Rasolomampionona, D. D. (2017). Next generation of power system protection automation—virtualization of protection systems. IEEE Transactions on Power Delivery, 33(4), 2002-2010.

[5] Guo, H. (2017). Time Synchronization and Communication Network Redundancy for Power Network Automation. The University of Manchester (United Kingdom).

[6] Kabbara, N., Nait Belaid, M. O., Gibescu, M., Camargo, L. R., Cantenot, J., Coste, T., ... & Morais, H. (2022). Towards software-defined protection, automation, and control in power systems: Concepts, state of the art, and future challenges. Energies, 15(24), 9362.

[7] Resch, J., Schuiki, B., Schöndorfer, S., Brandauer, C., Panholzer, G., Pröstl Andrén, F., & Strasser, T. I. (2020). Engineering and validation support framework for power system automation and control applications. e & i Elektrotechnik und Informationstechnik, 137(8), 470-475.

[8] Rajkumar, V. S., Tealane, M., Ştefanov, A., Presekal, A., & Palensky, P. (2020, October). Cyber attacks on power system automation and protection and impact analysis. In 2020 IEEE PES Innovative Smart Grid Technologies Europe (ISGT-Europe) (pp. 247-254). IEEE.

[9] Kulkarni, V., Sahoo, S. K., Thanikanti, S. B., Velpula, S., & Rathod, D. I. (2021). Power systems automation, communication, and information technologies for smart grid: A technical aspects review. TELKOMNIKA (Telecommunication Computing Electronics and Control), 19(3), 1017-1029.

[10] Heidari, S., Fotuhi-Firuzabad, M., & Lehtonen, M. (2017). Planning to equip the power distribution networks with automation system. IEEE Transactions on Power Systems, 32(5), 3451-3460.

[11] Northcote-Green, J., & Wilson, R. G. (2017). Control and automation of electrical power distribution systems. CRC press.

[12] Girón, C., Rodríguez, F. J., de Urtasum, L. G., & Borroy, S. (2018). Assessing the contribution of automation to the electric distribution network reliability. International Journal of Electrical Power & Energy Systems, 97, 120-126.

[13] Sarkar, S., Teo, Y. M., & Chang, E. C. (2022). A cybersecurity assessment framework for virtual operational technology in power system automation. Simulation Modelling Practice and Theory, 117, 102453.

[14] Sun, X., Zhou, Z., & Li, Z. (2021, June). Power automation system based on GPRS/CDMA wireless communication technology. In 2021 International Wireless Communications and Mobile Computing (IWCMC) (pp. 1988-1992). IEEE.

[15] Choi, I. S., Hong, J., & Kim, T. W. (2020). Multi-agent based cyber attack detection and mitigation for distribution automation system. IEEE Access, 8, 183495-183504.

[16] Rodríguez-Calvo, A., Cossent, R., & Frías, P. (2017). Assessing the potential of MV automation for distribution network reliability improvement. International Transactions on Electrical Energy Systems, 27(10), e2383.

[17] Sajadi, A., Strezoski, L., Strezoski, V., Prica, M., & Loparo, K. A. (2019). Integration of renewable energy systems and challenges for dynamics, control, and automation of electrical power systems. Wiley Interdisciplinary Reviews: Energy and Environment, 8(1), e321.

[18] Elkadeem, M. R., Alaam, M. A., & Azmy, A. (2017). Reliability improvement of power distribution systems using advanced distribution automation. Renewable Energy and Sustainable Development, 3(1), 24-32.

[19] Kamps, K., Möhrke, F., Zdrallek, M., Awater, P., & Schwan, M. (2020, August). Reliability of decentralized network automation systems and impacts on distribution network reliability. In 2020 International Conference on Probabilistic Methods Applied to Power Systems (PMAPS) (pp. 1-6). IEEE.

[20] Weijun Chen,Haiyan Yao,Xiaoling Yu & Hao Chen. (2024). Research on Differential Protection of Distribution Network Based on 5G Communication Technology. Journal of Physics: Conference Series(1),012016-012016.

[21] Sharma Ravi Shanker,Keswani Bright & Goyal Dinesh. (2022). Analysis of routing and security issues in OLSR protocol for video streaming over MANET. Journal of Discrete Mathematical Sciences and Cryptography(4),1203-1211.

[22] MoawiahEl Dalahmeh,AdiEl Dalahmeh & UsmanAdeel. (2024). Analysing the performance of AODV, OLSR, and DSDV routing protocols in VANET based on the ECIE method. IET Networks(5-6), 377-394.